JOURNAL OF CHEMICAL INFORMATION AND MODELING

Article

pubs.acs.org/jcim

Detecting Drug Promiscuity Using Gaussian Ensemble Screening

Violeta I. Pérez-Nueno,* Vishwesh Venkatraman, Lazaros Mavridis, and David W. Ritchie

INRIA Nancy − Grand Est, 615 rue du Jardin Botanique, 54506 Vandoeuvre-lès-Nancy, France

Supporting Information

ABSTRACT: Polypharmacology describes the binding of a ligand to multiple protein targets (a promiscuous ligand) or multiple diverse ligands binding to a given target (a promiscuous target). Pharmaceutical companies are discovering increasing numbers of both promiscuous drugs and drug targets. Hence, polypharmacology is now recognized as an important aspect of drug design. Here, we describe a new and fast way to predict polypharmacological relationships between drug classes quantitatively, which we call Gaussian Ensemble Screening (GES). This approach represents a cluster of molecules with similar spherical harmonic surface shapes as a Gaussian distribution with respect to a selected center molecule. Calculating the Gaussian overlap between pairs of such clusters allows the similarity between drug classes to be calculated analytically without requiring thousands of bootstrap comparisons, as in current promiscuity prediction approaches. We find that such cluster similarity scores also follow a Gaussian distribution. Hence, a cluster similarity score may be transformed into a probability value, or "p-value", in order to quantify the relationships between drug classes. We present results obtained when using the GES approach to predict relationships between drug classes in a subset of the MDL Drug Data Report (MDDR) database. Our results indicate that GES is a useful way to study polypharmacology relationships, and it could provide a novel way to propose new targets for drug repositioning.

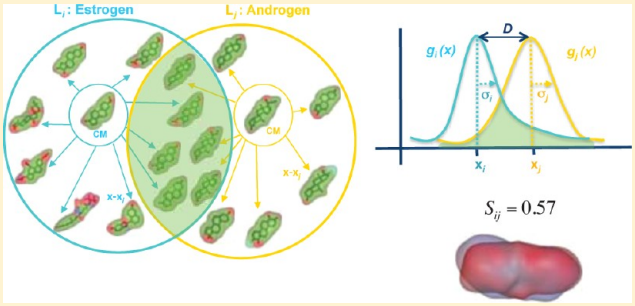

INTRODUCTION

Drug promiscuity may be defined as the pharmacological interaction of a given drug molecule with more than one biomolecular target. On the other hand, if a protein binds multiple different ligands, it can be considered as a promiscuous receptor.[1] The concept of "target-hopping," whereby a binder for one target can be considered as the basis for leads for another target, has historically been extremely fruitful in lead discovery.[2] Nowadays, the polypharmacology of promiscuous binders is recognized as an important aspect in drug design. For example, in the last four years, more than 30 drugs have been tested against more than 40 novel secondary targets on the basis of promiscuity predictions.[3] Furthermore, pharmaceutical companies are discovering increasing numbers of cases in which multiple drugs bind to a given target (promiscuous targets) and in which a given drug binds to more than one target (promiscuous ligands). Both of these phenomena are clearly of great importance when considering drug side effects. For example, a common reason for terminating a drug development program is that the leads are found to be nonselective or promiscuous.[4] Consequently, the in silico prediction of unwanted side effects caused by the promiscuous behavior of drugs and their targets is highly relevant to the pharmaceutical industry. Considerable effort is now being put into the computational[5,6] and experimental[7,8] screening of several suspected off-target proteins in the hope that side effects might be identified early, before the cost associated with developing a drug candidate rises steeply.[9] On the other hand, promiscuity is not always unwelcome, and it can even be exploited for drug development. The use of old drugs for new targets has been shown to provide a promising way to reduce both the time and cost of drug development.[10]

Although it would be desirable to be able to screen a drug against all proteins expressed by the human genome, this is currently infeasible. Therefore, several computational techniques have been developed to predict in silico the pharmacological profiles of known drugs. These range from conventional protein−ligand docking to the use of machine learning methods,[11,12] sequence comparison[13] side effect similarity,[6] and fingerprint/pharmacophore comparison methods.[14,15] These methods typically aim to relate protein receptors to each other quantitatively using their similarity in primary sequence space,[14] ligand chemical descriptor space,[15] and pharmacophoric pocket descriptor space.[16]

Recently, other approaches have been developed that compare the ligand chemistries of different targets on the assumption that similar molecules are likely to have similar properties.[17] For example, Mestres et al. relate proteins in ligand space using their in-house molecular descriptors (PHRAG, FPD, and SHED).[21,22] Their results confirm that the topology of drug−target networks depends implicitly on data completeness, drug properties, and target families. For example, from their analysis of drug properties, they observed that small hydrophobic drugs, which often interact primarily with GPCRs, appear to be significantly more promiscuous than

Received: February 20, 2012
Published: July 1, 2012

   dx.doi.org/10.1021/ci3000979 | J. Chem. Inf. Model. 2012, 52, 1948−1961

large hydrophilic drugs, which are often enzyme inhibitors.[22] Keiser et al. relate receptors to each other according to the chemical similarity of their ligands. In their Similarity Ensemble Approach (SEA),[18] the calculated probability that two molecules might interact with the same target by chance is expressed using an expectation value,[19] which is conceptually similar to the E-value used in sequence alignment software such as BLAST.[20]

Here, we describe a new and fast way to predict quantitatively the relationships between drug classes, which we call Gaussian Ensemble Screening (GES). In the GES approach, a cluster of molecules is represented as a Gaussian distribution with respect to a selected center molecule. By calculating the Gaussian overlap between pairs of such clusters, we can rapidly calculate the similarity between drug classes.[23] Thus, our approach provides a fast way of comparing target families without requiring thousands of bootstrap comparisons as in current promiscuity prediction approaches.[15] Furthermore, the observed distribution of the GES cluster overlap scores is also found to follow a Gaussian distribution. Hence, each Gaussian similarity score can readily be transformed into a probability value, or "p-value", in order to quantify the relationship between drug classes.

Here, we present the results of applying the GES approach to a wide range of ligands for some 270 specific drug classes that Schuffenhauer et al.[24] selected from the MDL Drug Data Report (MDDR) database in a previous study.[25] We compare our promiscuity predictions with those of SEA and with some experimental results reported by Keiser et al. for selected MDDR compounds. Overall, the GES approach finds interesting relationships between several targets, including relationships between, for example, GABA A and tyrosine-specific protein kinase, ACE and neutral endopeptidase, thromboxane antagonist and thromboxane synthetase inhibitor, dopamine reuptake inhibitor and norepinephrine uptake inhibitor, 5 HT reuptake inhibitor and 5 HT1A antagonist, PAF antagonist and lipoxygenase inhibitor, and also muscarinic M1 agonist and poly-(ADP-ribose) synthetase inhibitor. The polypharmacology of the latter pair has previously been confirmed experimentally. GES also detects other relationships that were previously predicted using SEA and which were subsequently confirmed in vitro by Keiser et al.

METHODS

Calculating Spherical Harmonic Shapes. Here, the PARASURF program is used to calculate from semiempirical quantum mechanics theory (using CEPOS Mopac[26] with the default Hamiltonian AM1) the molecular shape and the local surface properties of all ligands and to encode these properties as spherical harmonic (SH) expansions. PARAFIT is then used to superpose the SH molecular surfaces by exploiting the special rotational properties of the SH expansions.[26−31] The SH representation also provides a straightforward way to construct the average or "consensus" shape of a group of molecules by calculating the average of their SH expansion coefficients.[32] The consensus shape representation can be used to capture the essential 3D shape features of several known high-affinity ligands and to encode them in the form of a single representative pseudomolecule that may be used as a VS query. Furthermore, once a SH consensus shape has been calculated for a group of molecules, it is straightforward to use PARAFIT to identify the center molecule (CM), i.e., the real molecule whose SH surface is closest to that of the consensus shape.

Data Preparation. We extracted all ligands from version 2010.2 of the MDDR compound database,[25] which is a compilation of about 169,000 drug-like ligands in 663 activity classes and which annotates molecules by their therapeutic or biological category. Hence, a group of ligands that share an annotation define a set of functionally related molecules. However, many MDDR annotations are too general to be useful (e.g., "cancer vaccine", "sweetener", "pharmacological tool"). Therefore, in order to select a more specific subset of annotations, we used the ontology of Schuffenhauer et al.[24] that relates MDDR activity classes to Enzyme Commission (EC) numbers[33] and to known GPCRs, ion channels, and nuclear receptors, for example. This allowed a subset of ligands belonging to 270 specific annotations to be selected, as listed in Table 1 of the Supporting Information. Salts and other crystallization fragments were then removed, and ligand protonation states were normalized using LigPrep.[34] The lowest energy Corina[35] 3D conformations as supplied by MDDR version 2010.2 were used. After removing duplicate molecules, this gave a total of 77,801 distinct ligands with a median of 95 and a mean of 242 ligands per annotation. The SH molecular surface for each ligand was calculated using PARASURF. However, as noted by Sheridan et al.[36] and Keiser et al.,[18] MDDR annotations are quite general and were primarily derived from the patent literature. A given annotation may thus contain a diverse set of compounds with a wide range of affinities. Hence, in order to eliminate outliers, we used the CAST clustering algorithm[37] to cluster the members of each annotation using their PARAFIT Tanimoto similarity scores. We then calculated the consensus shape and the CM for each cluster, and we eliminated any cluster members beyond 1.5 standard deviations (SDs) from the corresponding CM. We call each of the resulting clusters a "ligand set".

Gaussian Ligand Set Comparisons. Because Gaussian functions require a distance coordinate rather than a similarity score, we used PARAFIT to calculate the normalized SH distance ($0.0 \le x \le 1.0$) between that of the CM and each cluster member that survived the above filter. Assuming that these distances follow a Gaussian distribution, each cluster may be represented as a probability density function $g_i(x)$

$$g_i(x) = \sqrt{\frac{1}{2\pi\sigma_i^2}} \cdot e^{(x-x_i)^2/2\sigma_i^2} \tag{1}$$

where $|x - x_i|$ represents the distance from the i^{th} CM, and σ_i is the SD of the member distances. A Hodgkin-like[38] similarity score S_{ij} between two distributions is then expressed as

$$s_{ij} = \frac{2\int_{-\infty}^{+\infty} g_i(x)\cdot g_j(x)\mathrm{d}x}{\int_{-\infty}^{+\infty} g_i(x)^2\mathrm{d}x + \int_{-\infty}^{+\infty} g_j(x)^2\mathrm{d}x} \tag{2}$$

The Gaussian overlap integrals can be simplified to a closed expression involving only the Gaussian widths and the distance between the CMs using standard techniques.[39] Putting $a = 1/(2\sigma_i^2)$ and $b = 1/(2\sigma_j^2)$, it can then be shown that

$$s_{ij} = \frac{2^{3/2}\cdot\left(\frac{a\cdot b}{a+b}\right)^{1/2}\cdot e^{-\left(\frac{a\cdot b}{a+b}\right)\cdot x_{ij}^2}}{(a^{1/2}+b^{1/2})} \tag{3}$$

dx.doi.org/10.1021/ci3000979 | J. Chem. Inf. Model. 2012, 52, 1948−1961

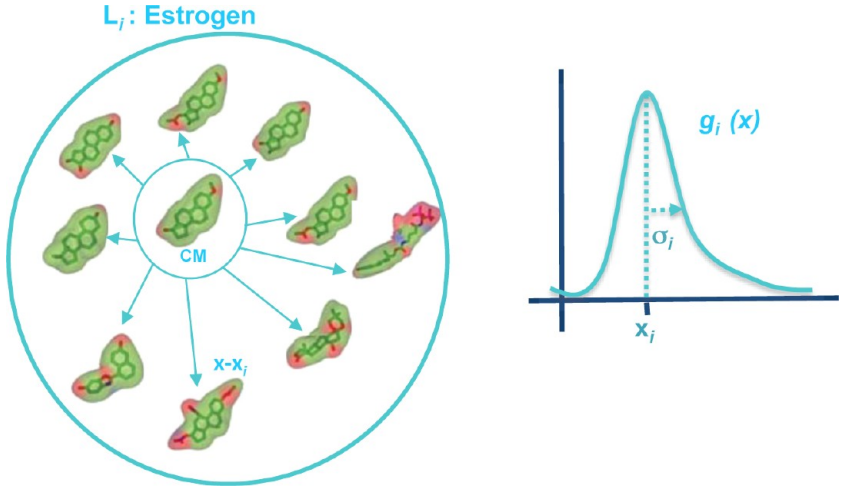

Figure 1. An illustration of a Gaussian ligand set cluster. A cluster of molecules (left) is represented as a Gaussian distribution (right) with respect to the center molecule (CM) of the cluster. As explained in the main text (see eq 1), the x axis represents a normalized SH distance (1-Parafit Tanimoto similarity score) between that of the CM and each cluster member. Assuming that these distances follow a Gaussian distribution, each cluster may be represented as a probability density function $g_i(x)$ (see eq 1), as illustrated on the right.

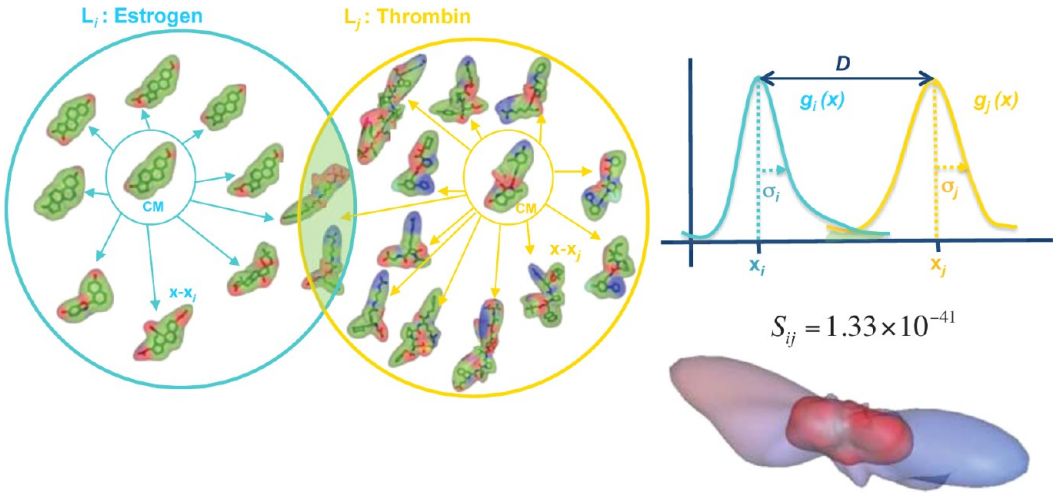

Figure 2. Illustration of the small Gaussian overlap between the estrogen and thrombin ligand sets. The similarity, S_{ij}, of two clusters is calculated from the overlap of their Gaussian distribution functions. By using the distance, D, between the corresponding center molecules and the standard deviation of each cluster (σ_i and σ_j), this similarity score may be calculated analytically (see eq 3). In this example, the small Gaussian overlap between the estrogen and thrombin ligand sets indicates that these drug classes are very unlikely to be related.

were x_{ij} is the distance between the CMs of clusters i and j. Thus, it is straightforward to calculate the values for all-v-all cluster comparisons. It is worth noting that this cluster similarity score depends only on the similarity of pairs of center molecules and the SDs of their respective clusters. Unlike the SEA approach, it does not depend on the number of members of each cluster.[18] Figure 1 shows schematically the calculation of the ligand set cluster for estrogen. Similarly, Figure 2 and Figure 3 illustrate the Gaussian overlap between the estrogen ligand set with the thrombin and androgen ligand sets, respectively.

Bootstrapping a Shape Clustering Similarity Threshold. Although the Gaussian model provides a straightforward way to compare clusters of molecules, we do not know a priori how best to form the initial clusters. Therefore, each ligand set was randomly split into two almost equal subclusters, and all-v-all clustering was performed on the subclusters using different similarity thresholds. All singleton clusters were ignored. Thus, starting from N clusters of presumably related ligands, this procedure produces $4N^2$ possible pairs of subclusters, of which at least N are assumed to be related and the rest are assumed to be unrelated. On the assumption that an ideal clustering threshold should generally rank the related pairs more highly than the unrelated pairs, the task of finding the best clustering threshold may be considered as a kind of virtual screening (VS) problem. More specifically, using a ranked list of $4N^2$ pairwise subcluster scores for each clustering threshold, the area under the curve (AUC) of a receiver-operator-characteristic (ROC) analysis may be used to identify the threshold that best recovers the correct pairs of subclusters. Figure 4 summarizes the overall procedure. However, as is often the case in real VS experiments, we assume that "early recognition" is important, and we therefore focus on the AUC of the first 5% and 10% of each ROC plot. Figures 1 and 2 of the Supporting Information show the ROC and the precision−recall (PR) curves, respectively, obtained for similarity thresholds of 0.6, 0.65, 0.675, 0.7, 0.8, and 0.85. These plots show that a PARAFIT Tanimoto similarity score of 0.65 optimizes both the area under the ROC

dx.doi.org/10.1021/ci3000979 | J. Chem. Inf. Model. 2012, 52, 1948−1961

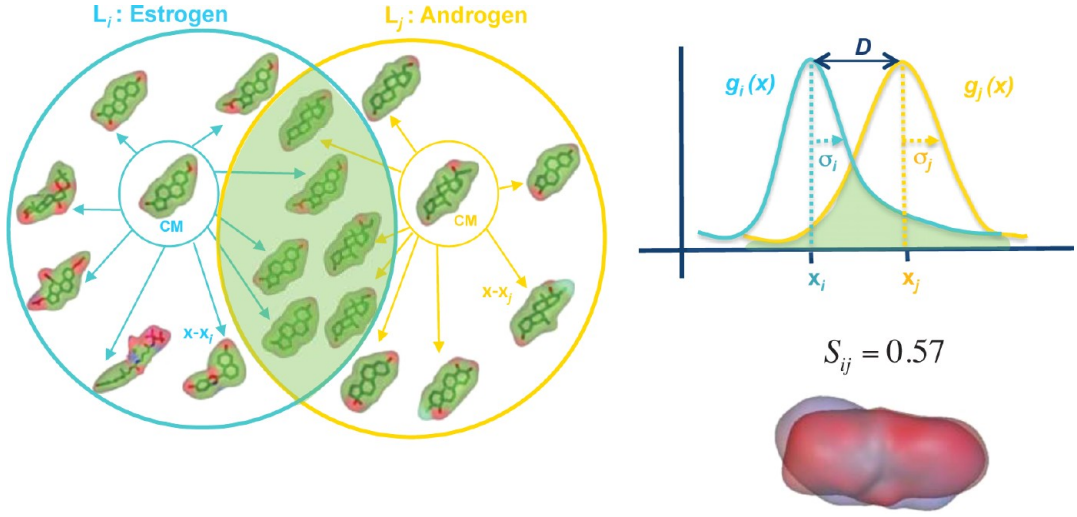

Figure 3. Illustration of the large Gaussian overlap between the estrogen and androgen ligand sets. In this example, the large Gaussian overlap between the estrogen and androgen ligand sets indicates that these drug classes might be related.

curve and the area under the PR curve. This threshold gave the best early ROC performance AUC (5%, 10%) and good precision and recall. Hence, using 0.65 as the clustering threshold gives the best VS-based recognition of the split clusters.

Gaussian p-Values. In order to transform a list of cluster similarity scores into a more meaningful list of probabilities, a simple statistical model was developed. First, using the ligand sets obtained above with a clustering Tanimoto threshold of 0.65, any outliers of each cluster were pruned. This was done by calculating the mean and SD of the Gaussian widths of all nonsingleton clusters and by pruning all cluster members further than 1.5 SD away from their corresponding CM. All singleton clusters were assigned the mean Gaussian width of the smallest observed SD. Each cluster CM was then recalculated without the outliers, and the all-*v*-all cluster comparison was repeated using the reduced clusters. We then used the R package[40] to fit the distribution of the obtained Gaussian cluster overlap scores to several statistical functions. This indicated that the distribution that best describes the observed distribution of these scores was again a Gaussian function. Thus, a p-value may be readily calculated from the scores distribution for any given pairwise score using the standard statistical techniques. For example, for a Gaussian distribution, it can be shown that the probability of finding at random from the distribution some value X greater than a given value x is given by

$$p(X > x) = \int_x^\infty f(t)\mathrm{d}t = \mathrm{erfc}(x) \tag{4}$$

where $f(t)$ is the standard normalized Gaussian probability density function and $\mathrm{erfc}(x)$ is the complementary error function. Hence, for a normalized distribution of scores, we obtain

$$p(S > s) = \mathrm{erfc}\left(\frac{s}{\sqrt{2\sigma^2}}\right) \tag{5}$$

where σ is the SD of the fitted Gaussian. In other words, for a given score, s, its p-value represents the probability of finding at random from the distribution some other score, S, which is greater than s. The plots in Figure 3 of the Supporting Information show the observed distribution of pairwise ligand set cluster scores plotted using 200 bins (Figure 3a, Supporting Information), the fitted Gaussian function with σ = 0.05274 (Figure 3b, Supporting Information), and the p-values calculated at each bin using the fitted distribution (Figure 3c, Supporting Information).

RESULTS

Similarity Scores between Ligand Sets. We used 270 specific annotations from the MDL Drug Data Report (MDDR), comprising a total of 77,801 ligands. Clustering each annotation using a PARAFIT shape Tanimoto similarity threshold of 0.65 gave a total of 321 annotation clusters (ligand sets), of which 37 contained singleton ligands. The similarity between each ligand set was calculated using the Gaussian overlap score as described in Methods. The results from the all-*v*-all ligand set comparisons were recorded as a matrix of GES p-values (the full matrix is available in Table 2, Supporting Information). We then extracted the 50 most significant relationships and also the top 50 relationships for each of the five main drug classes (nuclear hormone receptor, serine proteases, enzymes, GPCRs, and ion channels) to form six submatrices of the most interesting ligand set relationships.

MDDR Polypharmacology Interaction Matrix. Figure 5 shows the MDDR polypharmacology interaction matrix for the top 50 ligand set relationships calculated from the all-*v*-all comparison of the 270 specific annotations. The matrix is colored according to seven p-value intervals, ranging from orange ($p \leq 5 \times 10^{-60}$) to black ($p \geq 5 \times 10^{-10}$). Thus, a row of several orange elements could indicate a promiscuous target. Bearing in mind that this matrix represents entirely computational predictions, it can be seen that the GES algorithm strongly relates trypsin inhibitor, phosphodiesterase III inhibitor, thromboxane antagonist, 5 HT2C antagonist, TNF-α realase inhibitor, and protocollagen prolyl hydroxylase inhibitor to over 12 different targets. In particular, phosphodiesterase III inhibitor and protocollagen prolyl hydroxylase inhibitor are calculated to be the most promiscuous targets, being related to 22 and 14 different targets, respectively. Furthermore, poly-(ADP-ribose) synthetase inhibitor, adrenergic α1 blocker, 5HT1A antagonist, 5 HT2A antagonist, adenosine A2 antagonist, dopamine autoreceptor agonist,

dx.doi.org/10.1021/ci3000979 | J. Chem. Inf. Model. 2012, 52, 1948−1961

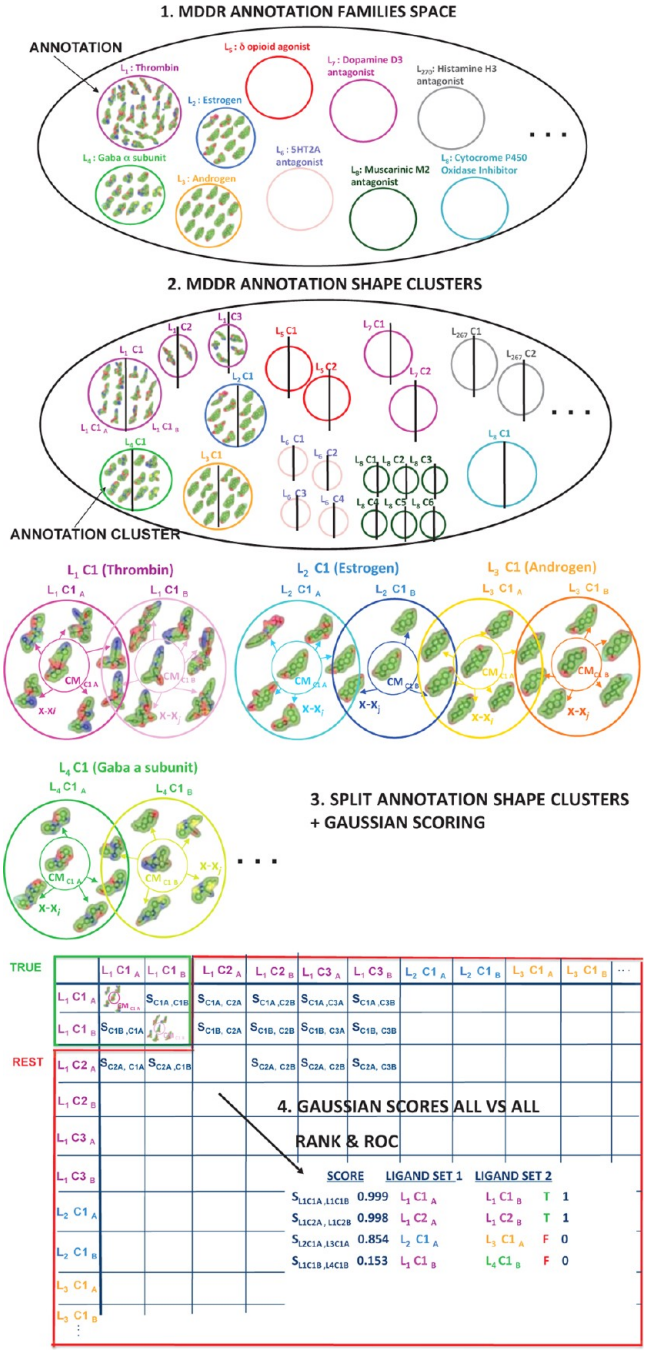

Figure 4. Schematic overview of the procedure used to determine a shape similarity threshold.

dopamine D2 agonist, tyrosine-specific protein kinase inhibitor, and benzodiazepine agonist/antagonist are strongly linked by GES to from 9 to 12 different targets.

Within the top 50 ligand set relationships, some very significant p-values are calculated for several well-known relationships, such as those between the antibiotics carbacephem and cephalosporin and between the steroid 5α reductase inhibitor and antiandrogen (several 5-α-reductase inhibitors are known to be antiandrogenic, as they prevent the reduction of testosterone to dihydrotestosterone[41]). Moreover, there exists experimental evidence to support some of the other strongly predicted relationships, such as those between the dopamine reuptake and norepinephrine uptake inhibitors,[42] TNF and IL-8 inhibitors (TNF inhibition causes IL-8 protein release[43,44]), leukotriene and VCAM-1 inhibitors (leukotriene synthesis inhibition is stimulated by VCAM-1 adhesion[45,46]), leukotriene D4 antagonists and leukotriene antagonists,[47] phosphatidylinositol kinase inhibitors and calpain inhibitors,[48] PAF antagonists and tyrosine−specific protein kinase inhibitors,[49] PAF antagonists and lipoxygenase inhibitors,[50] PAF antagonists and phosphodiesterase III inhibitors,[51] PAF antagonists and adenosine (A2) antagonists,[52] and between PAF antagonists and 5 HT antagonists.[53]

Figure 5 shows that GES also finds several interesting but undocumented relationships between leukotriene D4 antagonists, dopamine D3 antagonists, and leukotriene antagonists, and also between, for example, the GABA B and leukotriene antagonists, phosphatidylinositol kinase inhibitors and cyclooxygenase-1 inhibitors, gpIIb/IIIa receptor antagonists and leukotriene D4 antagonists, dopamine D3 antagonists and leukotriene antagonists, 5 HT1B agonists and 5 HT antagonists, PAF antagonists and 5 HT4 agonists, and between PAF antagonists and adrenergic α1 blockers.

In order to examine these predicted interactions in more detail, Figures 6−10, show the interaction submatrices for several strongly predicted relationships involving the selected five main MDDR drug classes. For example, the high numbers of orange, green, blue, and lilac elements in Figure 6 (nuclear hormone receptor inhibitors) show that estrogen, antiandrogen, and thyroid have significant relationships with other ligand sets. As noted above, antiandrogen is strongly predicted to be related to steroid 5α reductase inhibitor. Estrogen is predicted to be significantly related with adrenorecepor α2 antagonist, uridine phosphorylase inhibitor, dopamine autoreceptor agonist, 5 HT1A antagonist, protein kinase C inhibitor, IL-6 inhibitor, and phosphodiesterase III inhibitor. The thyroid inhibitor is predicted to be significantly related to adrenorecepor α2 antagonist and uridine phosphorylase inhibitor. Moreover, antiglucocorticoid is predicted to be closely related to progesterone antagonist (in agreement with experimental evidence for the antiglucocorticoid action of progesterone[54,55]), and parathyroid hormone antagonists are predicted to be related to vitamin D analogs and carbacephem (which is also supported by experimental information[56,57]).

Figure 7 (serine protease inhibitors) shows that tryptase, trypsin, elastase, prolyl endopeptidase, and chymotrypsin have strong predicted relationships with other ligand sets. For example, tryptase inhibitor is linked to trypsin inhibitor and 5 HT antagonist. Trypsin inhibitor is linked to 13 different targets. Prolyl endopeptidase inhibitor is linked to phosphodiesterase III inhibitor. Chymotrypsin inhibitor is strongly linked to 5 HT antagonist, VCAM-1 antagonist, carbacephem, and thrombin inhibitor (experimental information exists to support the last two relationships[58,59]). Moreover, factor VIIa inhibitor is linked to factor Xa inhibitor (in fact, the factor VII enzyme is activated to factor VIIa by different proteases, among which are thrombin factor IIa, and factor Xa).

Figure 8 (enzyme inhibitors) shows that tyrosine-specific protein kinase, acetylcholinesterase, nitric oxide synthase, and carbonic anhydrase also have strong links with other ligand sets. Indeed, tyrosine-specific protein kinase is calculated to be the most promiscuous enzyme, being strongly linked to nine different targets. Acetylcholinesterase inhibitor is strongly linked to six different targets. Among those links, some experimental information supports the relationship between lipoxygenase and acetylcholinesterase, i.e., there is experimental

dx.doi.org/10.1021/ci3000979 | J. Chem. Inf. Model. 2012, 52, 1948−1961

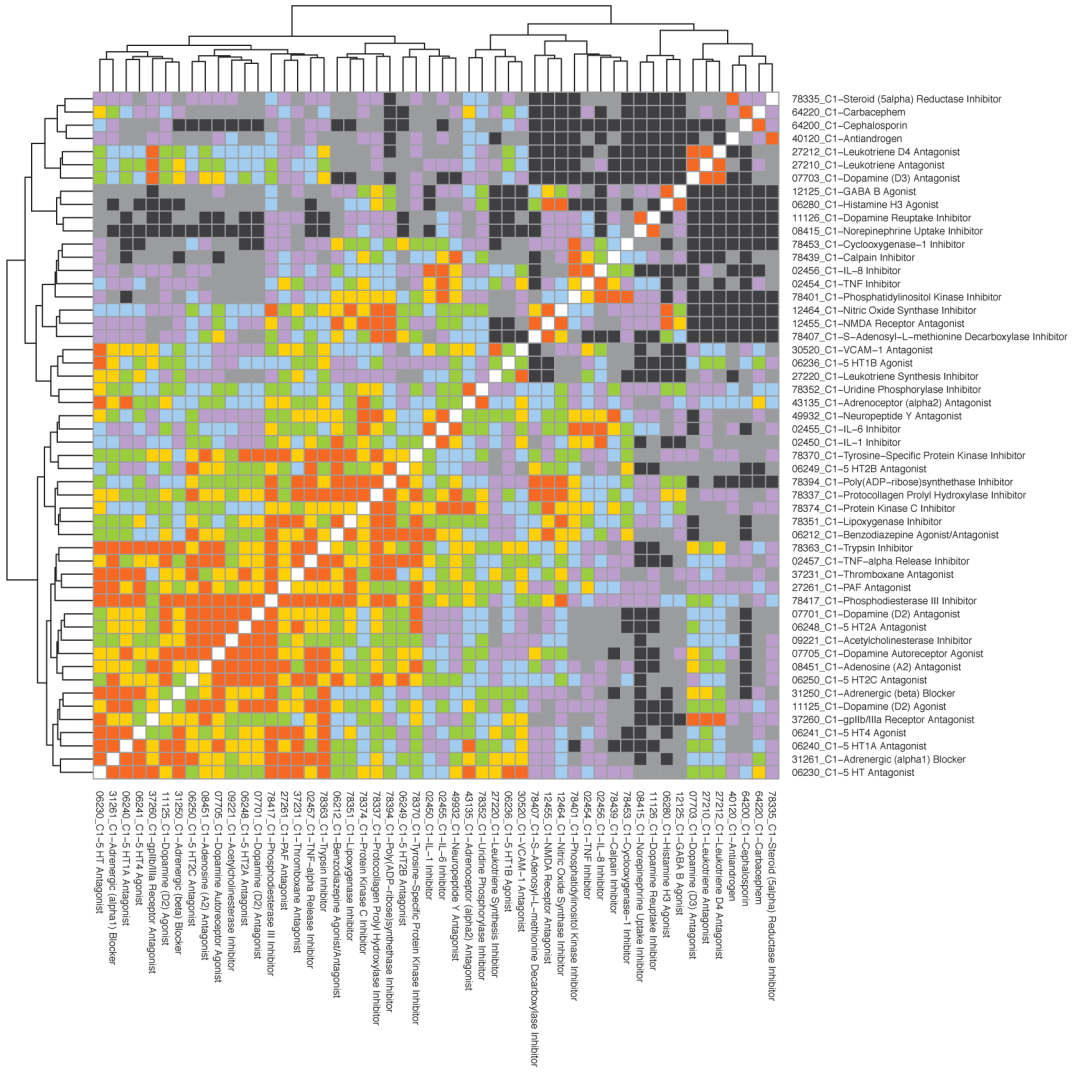

Figure 5. MDDR polypharmacology interaction matrix for the top 50 ligand set relationships found from the all against all comparison of the 270 MDDR specific annotations. The matrix elements are colored according to seven p-value ranges: $p \leq 5 \times 10^{-60}$ in orange; $5 \times 10^{-60} < p \leq 5 \times 10^{-50}$ in yellow; $5 \times 10^{-50} < p \leq 5 \times 10^{-40}$ in green $5 \times 10^{-40} < p \leq 5 \times 10^{-30}$ in blue; 5×10^{-30} < p-value $\leq 5 \times 10^{-20}$ in lilac; $5 \times 10^{-20} < p \leq 5 \times 10^{-10}$ in gray; and $p > 5 \times 10^{-10}$ in black. No p-value is calculated for a ligand set with itself (white elements).

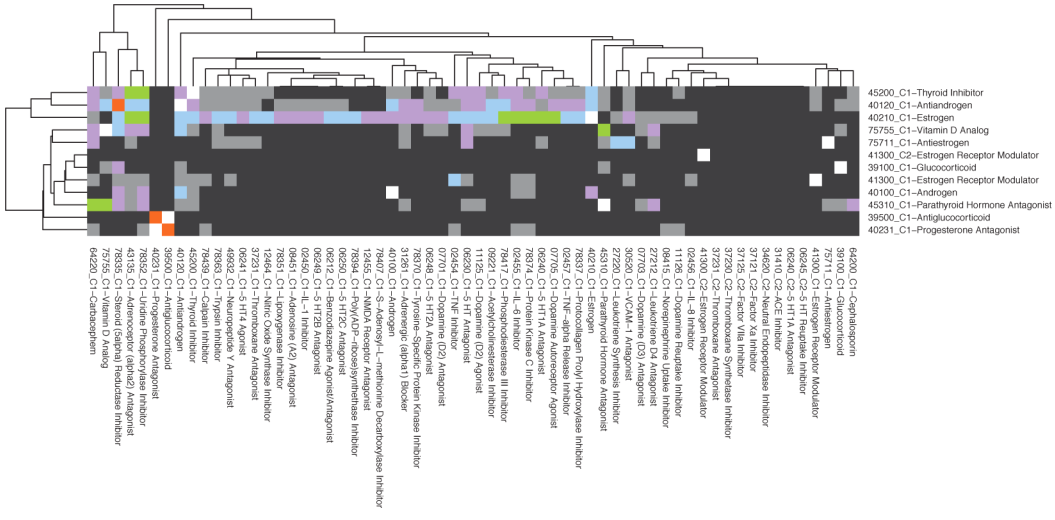

Figure 6. Subset of the MDDR interaction matrix involving several nuclear hormone receptors. See Figure 5 for details of the color scheme.

dx.doi.org/10.1021/ci3000979 | J. Chem. Inf. Model. 2012, 52, 1948−1961

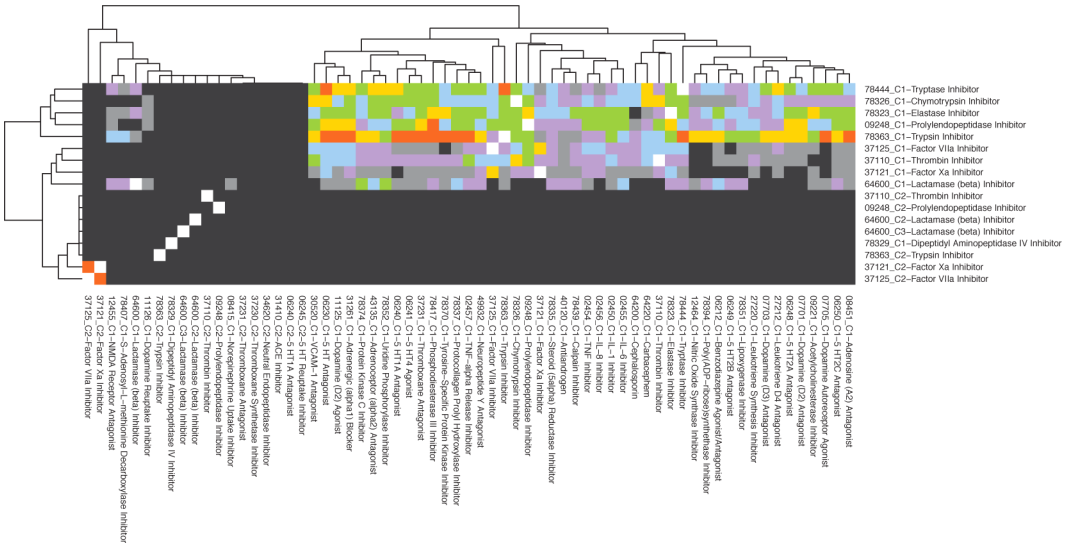

Figure 7. Subset of the MDDR interaction matrix involving several serine proteases. See Figure 5 for details of the color scheme.

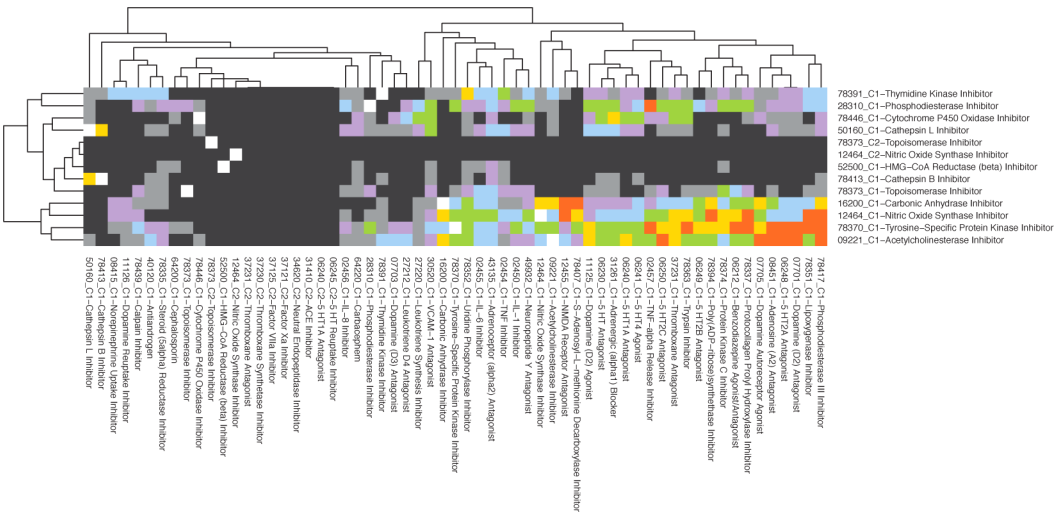

Figure 8. Subset of the MDDR interaction matrix involving several enzyme inhibitors. See Figure 5 for details of the color scheme.

evidence of anti-5-lipoxygenase and antiacetylcholinesterase activities of essential oils and decoction waters of some aromatic plants.[60] Additionally, for the dopamine D2 antagonist and acetylcholinesterase link, there is experimental evidence of anticholinesterase activity of dopamine D2 receptor antagonist.[61] Similarly, for the predicted relationship between 5-HT2C/5-HT2B antagonist and acetylcholinesterase, it is known that the acetylcholine release induced by a NK3 receptor agonist is inhibited by stimulation of a 5-HT receptor (possibly of the 5-HT2C or 5-HT2B subtype).[62] Furthermore, carbonic anhydrase inhibitor is strongly linked to NMDA receptor antagonist and S-adenosyl-L-methionine decarboxylase inhibitor. Nitric oxide synthase inhibitor is linked to phosphodiesterase III inhibitor, lipoxigenase inhibitor (which is consistent with existent experimental data[63]), protocollagen prolil hydroxylase inhibitor, NMDA receptor antagonist (which both act in a similar way[64]), and poly-(ADP-ribose) synthetase inhibitor (there is experimental evidence that nitric oxide synthase is responsible for poly-(ADP-ribose) synthetase activation[65]). Finally, cathepsin B and cathepsin L inhibitors are also strongly linked. This is not unexpected, given that both are cysteine proteases and are known to act similarly.[66]

Figure 9 (GPCR inhibitors) shows that dopamine D2 antagonist, 5 HT2A antagonist, dopamine D2 agonist, 5 HT2C antagonist, adrenergic α1 blocker, 5 HT4 agonist, 5 HT1A antagonist, 5 HT2B antagonist, and 5 HT1D agonist are all linked with several ligand sets. Moreover, muscarinic M2 antagonist is strongly linked with dopamine D3 antagonist, and both are also strongly linked to leukotriene D4 antagonist. Among the top 50 predicted relationships are muscarinic M1 agonist and histamine H3 agonist with nitric oxide synthase inhibitor and NMDA receptor antagonist, which are supported by experimental evidence.[67−69] Also, 5 HT reuptake inhibitor is strongly linked to 5 HT1A antagonist, and muscarinic M1 agonist is strongly linked to poly-(ADP-ribose) synthetase inhibitor. Both of these relationships agree with existing dual inhibitors for these targets.[70−72] Moreover, preclinical studies show that selective 5-HT1A receptor antagonists potentiate the effect of 5 HT reuptake inhibitors.[73,74]

Figure 10 (ion channel inhibitors) shows that the GABA B agonist, GABA transaminase inhibitor, and GABA A/benzodiazepine receptor complex-related drug each have relationships with several other ligand sets, with GABA A being predicted to be the most promiscuous (related to four

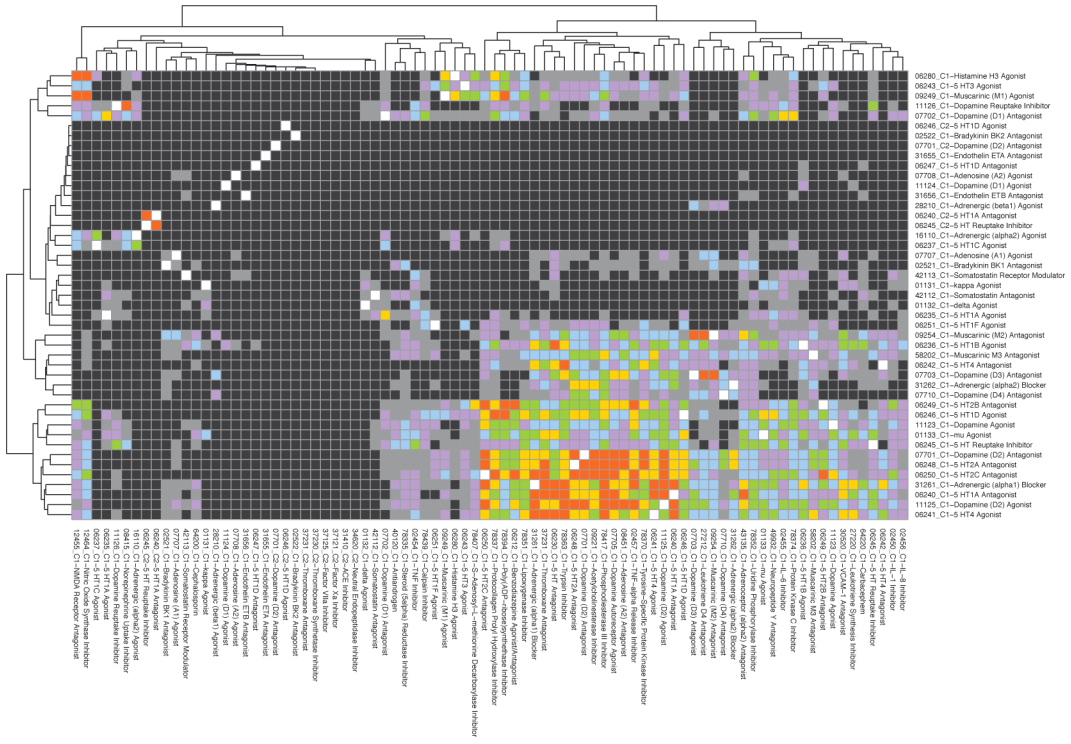

Figure 9. Subset of the MDDR interaction matrix involving several GPCRs. See Figure 5 for details of the color scheme.

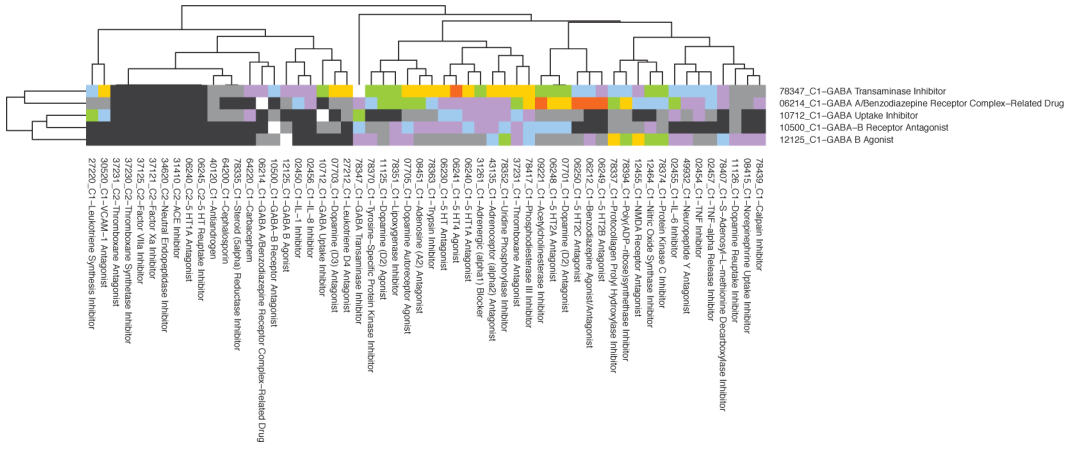

Figure 10. Subset of the MDDR interaction matrix involving several ion channels. See Figure 5 for details of the color scheme.

different targets). GABA transaminase inhibitor is predicted to be highly significantly related with 5 HT4 agonist, which is confirmed by experimental evidence.[75,76] GABA A is predicted to be strongly related with acetylcholinesterase inhibitor, which is confirmed by experimental evidence of dual inhibitors such as bis(7)-tacrine.[77] GABA A is also predicted to be strongly linked to the 5 HT2B antagonist, benzodiazepine agonist/antagonist, and 5 HT2C antagonist, which is also supported by experimental information.[78−81]

Figure 11 shows some examples of the SH shape superpositions of the CMs of some of the strongly linked ligand sets discussed above, namely, the IL-8 inhibitor and TNF inhibitor, VCAM-1 antagonist and leukotriene synthesis inhibitor, carbacephem and cephalosporin, steroid 5α reductase inhibitor and antiandrogen, dopamine reuptake inhibitor and norepinephrine uptake inhibitor, muscarinic M1 agonist and poly-(ADP-ribose) synthetase inhibitor, muscarinic M1 agonist and nitric oxide synthase inhibitor, GABA A and benzodiazepine agonist/antagonist, GABA A and acetylcholinesterase inhibitor, and progesterone antagonist and antiglucocorticoid. It can be seen that the CM ligands of these ligand sets have very similar SH shapes.

Comparison with SEA and Experimental Evidence. Table 1 shows a comparison of the promiscuity predictions obtained by GES for the five MDDR activity classes with the results reported previously by Keiser et al.[18] However, because our approach represents and groups ligands using smooth analytic functions whereas SEA uses combinatorial sampling of 2D fingerprints, it is not appropriate to compare absolute scores or p-values directly. Nonetheless, it is useful to compare the relative rank obtained for the compounds in each ligand set. In this respect, Table 1 shows that GES finds in the first ranking positions the same one or two related ligand sets as the SEA algorithm. Given that SEA uses 2D Daylight fingerprints while

dx.doi.org/10.1021/ci3000979 | J. Chem. Inf. Model. 2012, 52, 1948−1961

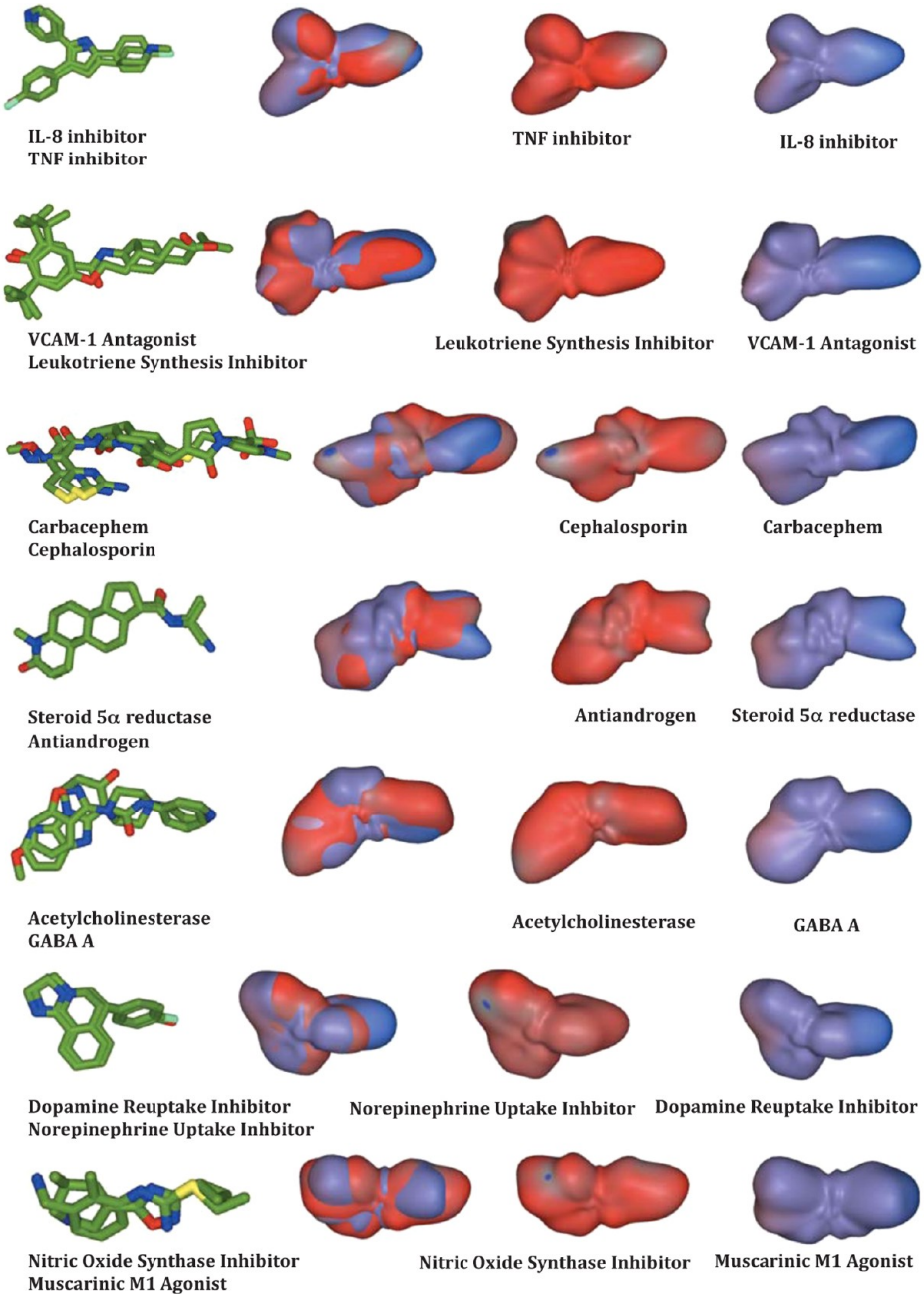

Figure 11. Examples of SH shape superpositions of the CMs of some of the strongly related targets found in the selected MDDR subset.

GES uses 3D SH shape representations, the overall similarity of the results in Table 1 is rather remarkable. Indeed, further comparing our GES promiscuity predictions with those of Keiser et al. shows that, like SEA, GES also predicts that the serotonin reuptake inhibitors might inhibit uptake of serotonin into presynaptic neurons and that these inhibitors could also act as β-blockers (which bind to β-adrenergic receptors in, e.g., blood vessels and heart muscle). These predictions were confirmed in vitro by Keiser et al.[18] However, there are also several targets that the GES surface-based technique relates with significant p-values but that SEA does not (Table 1), such as AMPA and phosphatidylinositol, chymotrypsin and carbacephem, 5 HTF 1 agonist and mGlu1, and adrenergic beta1 agonist and squalene epoxidase inhibitor. In particular, GES relates GABA A and 5HT1F agonist with a significant p-value while SEA does not, yet there is experimental evidence of this relationship.[82]

The GES approach also finds a strong link between 5 HT reuptake inhibitor and adrenergic β-blocker ($p = 10^{-41}$) and also a possible link between 5 HT reuptake inhibitor and adrenergic $\beta 1$ blocker ($p = 10^{-20}$). This could suggest that some of the side effects that occur when patients stop taking serotonin reuptake inhibitor antidepressants might be caused by a rebound in β-adrenergic signaling. Because the serotonin and β-adrenergic receptors bind to chemically similar naturally occurring ligands, the predicted β-blocker activity of the serotonin reuptake inhibitors might not be so surprising.

On the other hand, a much tougher challenge is to predict a compound's polypharmacology for drug targets that share no discernible similarity in amino acid sequence, protein structure, or endogenous ligands. Like the SEA approach, GES can also

Table 1. Most Significant GES Relationships Found Involving Five Example MDDR Activity Classes and Comparison with Results from SEA

	GES Rank	GES p-value	Ligands	Activity Classes	SEA Rank	SEA E-value	Experimental evidence
AMPA Receptor Antagonist	1	0[a]	536	AMPA receptor antagonist	1	2.45×10^{-290}	✓
	2	5.23×10^{-62}	327	Phosphatidylinositol Kinase inhibitor			
	3	6.12×10^{-61}	358	Poly-(ADP-ribose) synthethase Inhibitor			
	4	1.40×10^{-59}	303	Adenosine (A1) Antagonist			
	5	2.97×10^{-57}	1431	NMDA Receptor Antagonist	3	3.08×10^{-63}	✓
	6	9.38×10^{-55}	530	Protein Kinase C Inhibitor			
Carbacephem	1	0[a]	102	Carbacephem	1	0[b]	✓
	2	5.91×10^{-72}	1221	Cephalosporin	2	1.11×10^{-222}	
	3	1.52×10^{-54}	10	Chymotrypsin Inhibitor			
	4	6.63×10^{-52}	39	5 HT Antagonist			
	5	7.47×10^{-52}	181	Tryptase Inhibitor			
	6	2.79×10^{-50}	24	Adrenoceptor (alpha2) Antagonist			
	7	6.04×10^{-47}	50	5 HT1B Agonist			
	8	5.38×10^{-46}	48	Phospholipase C Inhibitor			
Androgen	1	0[a]	15	Androgen	1	0[b]	✓
	2	7.52×10^{-61}	153	Aldosterone Antagonist	11	5.25e-4	
	3	1.44×10^{-60}	596	Aromatase Inhibitor	2	6.87×10^{-307}	✓
	4	6.14×10^{-39}	14	Steroid (5alpha) Reductase 1			
	5	1.09×10^{-37}	39	Progestin	4	9.92e-73	
	6	1.03×10^{-36}	208	Antiandrogen	6	1.14×10^{-70}	
	7	3.96×10^{-29}	756	Steroid (5alpha) Reductase Inhibitor	5	1.58×10^{-72}	✓
	8	4.80×10^{-27}	167	Estrogen	3	9.97×10^{-89}	✓
	9	3.22×10^{-25}	1020	HIV-1 Protease Inhibitor	22	1.66×10^{-03}	
	10	2.21×10^{-22}	1032	Reverse Transcriptase Inhibitor			
	11	7.47×10^{-22}	234	Lactamase (beta) Inhibitor			
5 HT1F Agonist	1	0[a]	1	5 HT1F Agonist	1	0[b]	✓
	2	1.15×10^{-44}	139	mGlu1 Antagonist			
	3	4.16×10^{-35}	491	GABA A/Benzodiazepine Receptor Complex			✓
	4	2.54×10^{-33}	60	Calpain Inhibitor			
	5	6.43×10^{-33}	559	Elastase Inhibitor			
	6	9.32×10^{-33}	773	H+/K+-ATPase Inhibitor			
	7	1.11×10^{-31}	1062	Tyrosine-Specific Protein Kinase Inhibitor			
	8	1.30×10^{-31}	640	5 HT1D Agonist	2	8.08×10^{-38}	✓
Adrenergic (β1) Agonist	1	0[a]	1	Adrenergic (β1) Agonist	1	0[b]	✓
	2	5.16×10^{-47}	110	Squalene Epoxidase Inhibitor			
	3	3.86×10^{-38}	313	Dopamine (D3) Antagonist			
	4	2.11×10^{-37}	30	Glycinamide Ribonucleotide			
	5	3.86×10^{-37}	384	Adrenergic (beta) Agonist	2	9.50×10^{-34}	
	6	1.47×10^{-35}	65	Adrenergic (beta1) Blocker	3	4.99×10^{-32}	
	7	2.61×10^{-27}	71	Muscarinic (M2) Antagonist			
	8	3.76×10^{-25}	74	Cholesterol Esterase Inhibitor			
	9	9.35×10^{-22}	639	Dopamine (D4) Antagonist			
	10	5.03×10^{-20}	613	Histamine			

[a] p-value < 10^{-80}; [b] E-value < 10^{-320}

relate drug targets having no obvious biological similarity. For example, GES finds a possible relationship between reverse transcriptase and histamine H3 ($p = 10^{-20}$). This might explain why anti-HIV reverse transcriptase medications sometimes cause painful skin rashes as a side effect.

Table 2 shows some examples of off-target interactions for the MDDR activity classes shown in Table 1 and for the activity classes with the most significant GES p-values that were found by manual literature search. This table summarizes how our predictions match the currently known affinity data for these drugs. The biological information was extracted from Binding DB, ChEMBL, and DrugBank databases. For these cases, it is shown that the highest related targets found by GES approach are confirmed by experimental information. However, it is difficult to make firm conclusions about the predictive power of our approach on the basis of the few examples for which we were able to find supporting experimental evidence.

■ DISCUSSION

We have shown that several therapeutic protein targets may be related quantitatively by calculating a ligand set interaction p-value matrix from the Gaussian overlap between shape-based

dx.doi.org/10.1021/ci3000979 | J. Chem. Inf. Model. 2012, 52, 1948−1961

Table 2. Drug off-Target Interactions for the MDDR Activity Classes Shown in Table 1 and the Activity Classes with the Most Significant GES p-Values That Were Found by Manual Literature Search. PMID Refers to PubMed ID

GES p-value	Compound	Known activities	Predicted target	PMID	Additional information	Drug SMILES
1.44E-60	MDDR Modelname 322945	Androgen	Aromatase inhibitor	8176709 1708928		O=C1CC[C@@H]2[C@@H]3[C@@H](C@H]4C[C@@H]5C[C@]5(CO)[C@]4(CC3)C)[C@@H](CC2=C1)C
2.97E-57	CNQX	AMPA receptor antagonist	Glutamate-NMDA-MK801	8558460	Ki (nM) = 5600	O=C1NC2=C(C#N)C([N+](=O)[O-])=CC2NC1=O
6.14E-39	MDDR Modelname 322945	Androgen	Steroid 5-alpha-reductase 1	7739004	IC50 (nM) = 2700	O=C1CC[C@@H]2[C@@H]3[C@@H](C@H]4C[C@@H]5C[C@]5(CO)[C@]4(CC3)C)[C@@H](CC2=C1)C
4.16E-35	MDDR Modelname LY-344864	5HT1F	GABA A/Benzodiazepine	9395253	Ki (nM) >10000.0	Fc1ccc(cc1)C(=O)Nc1cc2c3C[C@H](NC)C)CCC3)nH]c2cc1
1.30E-31	MDDR Modelname LY-344864	5HT1F	5 HT 1D agonist	11708905 9986723	Ki 1620 nM for compound in PMID 11708905 Ki 4.4 nM for compound in PMID 9986723	Fc1ccc(cc1)C(=O)Nc1cc2c3C[C@H](NC)C)CCC3)nH]c2cc1
4.80E-27	MDDR Modelname 322945	Androgen	Estrogen Receptor (ER-alpha)	16309907 17448656 15887952	IC50 (nM) > 100000 for compounds in PMID 17448656 and PMID 17890084 EC50/IC50 > 1000 for compounds in PMID 17448656 and PMID 15887952	O=C1CC[C@@H]2[C@@H]3[C@@H](C@H]4C[C@@H]5C[C@]5(CO)[C@]4(CC3)C)[C@@H](CC2=C1)C
1.41E-79	MDDR Modelname 142025	Norepinephrine Uptake inhibitor	Dopamine Transporter (DAT) (Dopamine reuptake inhibitor)	17489581	IC50(nM)=8800	c1(C[C@@H](NCCC)CCC)ccccc1
3.17E-78	MDDR Modelname 144046	Antiandrogen	Steroid 5-alpha-reductase 1/2	9873464 3783591	Ki 54.7 nM for compound in PMID 9873464 IC50 6.8 nM for compound in 3783591	[C@H]12[C@H]3[C@@H]([C@@H](C[C@@]4([C@@H](CC3)NC(=O)C=C4)C)CC[C@@]1([C@H](CC2)C(=O)OC)C

ligand set clusters. Our GES approach can identify both expected and unexpected similarities, which may be investigated by examining the known off-target activities of the ligands themselves. We have shown some specific examples in which GES can detect known promiscuous targets such as adrenergic α1 blocker, phosphodiesterase III inhibitor, thromboxane antagonist, and protocollagen prolyl hydroxylase inhibitor. It is worth noting that the center molecules of these targets' ligand sets are small and contain fused aromatic rings, which is a characteristic of promiscuous compounds.[22] Moreover, these targets have large and quite hydrophobic binding sites, which is also a common characteristic of promiscuity.[83]

Overall, we have presented a new approach to detect promiscuous ligands and targets. We have compared it with the earlier SEA promiscuity prediction approach, and we have validated it using available experimental information. The GES approach can find interesting relationships between targets such as GABA A and tyrosine-specific protein kinase, ACE and neutral endopeptidase, thromboxane antagonist and thromboxane synthetase inhibitor, dopamine reuptake inhibitor and norepinephrine uptake inhibitor, 5 HT reuptake inhibitor and 5 HT1A antagonist, PAF antagonist and lipoxygenase inhibitor, and also between muscarinic M1 agonist and poly-(ADP-ribose) synthetase inhibitor, for example, whose dual inhibitors have been experimentally confirmed[84−89,70,50,71] or for which there is experimental evidence for inhibitors acting on both identified related targets, such as 5 HT2A agonists and NMDA antagonists[90] or thromboxane antagonists and thromboxane synthetase inhibitors.[66] The GES approach also detects other expected similarities between, for example, the AMPA and NMDA receptor antagonists (both are glutamate receptors), carbacephem and cephalosporin (carbacephem antibiotic is synthetically made on the basis of the structure of cephalosporin), androgen and aromatase inhibitor (aromatase inhibitors work by inhibiting the action of the enzyme aromatase, which converts androgens into estrogens), 5HT1F and 5HT1D agonists (both are serotonin receptors), GABA A and 5HT2B or 5HT2C (serotonin receptors modulate the release of many neurotransmitters, including GABA,[78]), GABA A and benzodiazepine receptor complex (GABA A is also the molecular target of the benzodiazepine class of tranquilizer drugs), or between adrenergic β1 agonists and adrenergic β1 blockers (both are adrenergic receptors).

Although the GES clustering protocol presented here used 3D SH shapes as its starting point, we expect that it could equally be used to represent and compare the distributions of other molecular properties and similarity measures. All that is required is a way to identify a center molecule and to calculate a Gaussian width for each cluster. As shown here, calculating the Gaussian overlap between pairs of such distributions would allow the overall similarity between ensembles of attributes to be transformed into a p-value. Indeed, we believe that Gaussian ensembles could even be used to represent multiple ligand conformations and to analyze VS hit lists. For example, the conformations of a molecule could be represented as a Gaussian distribution with respect to a chosen center conformation, and the Gaussian similarity between ensembles of conformations could be transformed into a p-value in order to assign confidence levels to compounds in a ranked hit-list. Thus, using clusters of conformations could circumvent the difficult problem of how to select the best ligand conformation to use in current VS protocols. This is an important feature of our method given the high dependency of the results obtained

by ligand-based approaches on the particular 3D conformation shape. Indeed, using combinations of such Gaussian representations could provide a more rational way to select compounds for testing in a chemogenomic context than simply selecting a given percentage of hits. Hence, we propose that taking into account potential polypharmacology relationships between ligands seems to provides a promising way to identify new targets for existing drug molecules, and that using ensemble-based approaches could improve the ability of VS protocols to select better molecular candidates for drug development.

CONCLUSION

GES is a new 3D shape-based approach for predicting and quantifying drug promiscuity by correlating Gaussian clusters of ligand SH shapes. The method has been validated using drug ligand sets of the MDDR and has been demonstrated to be effective in identifying drug families that are known to have related MDDR activity classes. Our results show that GES provides an efficient way to measure the similarity between clusters of arbitrary numbers of members. Furthermore, we propose the GES approach could be extended to represent and compare distributions of other molecular attributes such as their 3D conformations. The examples presented here demonstrate that GES provides a useful way to explore polypharmacology relationships and that it could provide a novel way to propose new targets for drug repositioning.

ASSOCIATED CONTENT

Supporting Information

Tables: MDDR specific ligand set annotations used in the promiscuity predictions and full matrix of GES p-values for the all against all comparison of the 270 specific annotations. Figures: ROC-based and precision-recall analyses of the VS recognition of split MDDR clusters and statistical model of the MDDR ligand set cluster overlap scores. This material is available free of charge via the Internet at http://pubs.acs.org.

AUTHOR INFORMATION

Corresponding Author

*E-mail: violeta.pereznueno@inria.fr. Tel: + +33-3-83593045. Fax: + +33-3-83413079.

Notes

The authors declare no competing financial interest.

ACKNOWLEDGMENTS

The authors thank Cepos Insilico Ltd. for providing an Academic Licence for PARASURF. V.I.P.N. is grateful for a Marie Curie IEF Fellowship, grant reference DOVSA 254128.

REFERENCES

(1) Xie, L.; Xie, L.; Bourne, P. E. Structure-based systems biology for analyzing off-target binding. *Curr. Opin. Struct. Biol.* **2011**, *21*, 189−99.
(2) Wermuth, C. G. Selective optimization of side activities: Another way for drug discovery. *J. Med. Chem.* **2004**, *47*, 1303−1314.
(3) Keiser, M. J; Irwin, J. J.; Shoichet, B. K. The chemical basis of pharmacology. *Biochemistry* **2010**, *49*, 10267−10276.
(4) Azzaoui, K.; Hamon, J.; Faller, B.; Whitebread, S.; Jacoby, E.; Bender, A.; Jenkins, J. L.; Urban, L. Modeling promiscuity based on in vitro safety pharmacology profiling data. *ChemMedChem* **2007**, *2*, 874−880.
(5) Merlot, C. In silico methods for early toxicity assessment. *Curr. Opin. Drug Discovery Dev.* **2008**, *11*, 80−85.
(6) Campillos, M.; Kuhn, M.; Gavin, A. C.; Jensen, L. J.; Bork, P. Drug target identification using side-effect similarity. *Science* **2008**, *321*, 263−266.
(7) Fedorov, O.; Marsden, B.; Pogacic, V.; Rellos, P.; Müller, S.; Bullock, A. N.; Schwaller, J.; Sundström, M.; Knapp, S. A systematic interaction map of validated kinase inhibitors with Ser/Thr kinases. *Proc. Natl. Acad. Sci. U.S.A* **2007**, *104*, 20523−20528.
(8) Trubetskoy, O. V.; Finel, M.; Kurkela, M.; Fitzgerald, M.; Peters, N. R.; Hoffman, F. M.; Trubetskoy, V. S. High throughput screening assay for UDP-glucuronosyltransferase 1A1 glucuronidation profiling. *Assay Drug Dev. Technol.* **2007**, *5*, 343−354.
(9) Nobeli, I.; Favia, A. D.; Thornton, J. M. Protein promiscuity and its implications for biotechnology. *Nat. Biotechnol.* **2009**, *27*, 157−167.
(10) Chong, C. R.; Sullivan, D. J. New uses for old drugs. *Nature* **2007**, *448*, 645−646.
(11) Nigsch, F.; Bender, A.; Jenkins, J. L.; Mitchell, J. B. O. Ligand-target prediction using Winnow and naive Bayesian algorithms and the implications of overall performance statistics. *J. Chem. Inf. Model.* **2008**, *48*, 2313−2325.
(12) Niijima, S.; Yabuuchi, H.; Okuno, Y. Cross-target view to feature selection: identification of molecular interaction features in ligand−target space. *J. Chem. Inf. Model.* **2011**, *51*, 15−24.
(13) Paolini, G. V.; Shapland, R. H. B.; van Hoorn, W. P.; Mason, J. S.; Hopkins, A. L. Global Mapping of Pharmacological Space. *Nat. Biotechnol.* **2006**, *24*, 805−815.
(14) Weskamp, N.; Hüllermeier, E; Klebe, G. Merging chemical and biological space: Structural mapping of enzyme binding pocket space. *Proteins* **2009**, *76*, 317−330.
(15) Keiser, M. J.; et al. Predicting new molecular targets for known drugs. *Nature* **2009**, *462*, 175−181.
(16) Milletti, F.; Vulpetti, A. Binding pocket comparison using four-point pharmacophoric descriptors based on GRID. *J. Chem. Inf. Model.* **2010**, *50*, 1418−1431.
(17) Johnson, M. A.; Maggiora, G. M. *Concepts and Applications of Molecular Similarity*; John Wiley and Sons: New York, 1990.
(18) Keiser, M. J.; et al. Relating protein pharmacology by ligand chemistry. *Nat. Biotechnol.* **2007**, *25*, 197−206.
(19) Hert, J.; Keiser, M. J.; Irwin, J. J.; Oprea, T. I.; Shoichet, B. K. Quantifying the relationships among drug classes. *J. Chem. Inf. Model.* **2008**, *48*, 755−765.
(20) Altschul, S. A.; Gish, W.; Miller, W.; Myers, E. W.; Lipman, D. J. Basic local alignment search tool. *J. Mol. Biol.* **1990**, *215*, 403−410.
(21) Vidal, D.; Mestres. In silico receptorome screening of antipsychotic drugs. *J. Mol. Inf.* **2010**, *29*, 543−551.
(22) Mestres, J.; Gregori-Puigjané, E.; Valverde, S.; Solé, R. V. The topology of drug-target interaction networks: Implicit dependence on drug properties and target families. *Mol. BioSyst.* **2009**, *5*, 1051−1057.
(23) Pérez-Nueno, V. I.; Venkatraman, V.; Mavridis, L.; Ritchie, D. W. Predicting drug promiscuity using spherical harmonic surface shape-based similarity comparisons. *Open Conf. Proc. Journal* **2011**, *2*, 113−129.
(24) Schuffenhauer, A.; Zimmermann, J.; Stoop, R.; van der Vyver, J.-J.; Lecchini, L.; Jacoby, E. An ontology for pharmaceutical ligands and its application for in silico screening and library design. *J. Chem. Inf. Comput. Sci.* **2002**, *42*, 947−955.
(25) *MDL Drug Data Report*, 2010.2, Accelrys, Inc., San Diego, CA (USA), 2010.
(26) CEPOS In Silico Ltd. Erlangen, Germany, 2009. http://www.ceposinsilico.de/ (accessed December 13, 2011).
(27) Lin, J.; Clark, T. An analytical, variable resolution, complete description of static molecules and their intermolecular binding properties. *J. Chem. Inf. Model.* **2005**, *45*, 1010−1016.
(28) Mavridis, L.; Hudson, B. D.; Ritchie, D. W. Toward high throughput 3D virtual screening using spherical harmonic surface representations. *J. Chem. Inf. Model.* **2007**, *47*, 1787−1796.
(29) Pérez-Nueno, V. I.; Venkatraman, V.; Mavridis, L.; Clark, T; Ritchie, D. W. Using spherical harmonic surface property representations for ligand-based virtual screening. *Mol. Inf.* **2010**, *30*, 151−159.

(30) Pérez-Nueno, V. I.; Ritchie, D. W.; Rabal, O.; Pascual, R.; Borrell, J. I.; Teixidó, J. Comparison of ligand-based and receptor-based virtual screening of HIV entry inhibitors for the CXCR4 and CCR5 receptors using 3D ligand shape matching and ligand-receptor docking. *J. Chem. Inf. Model.* **2008**, *48*, 509−533.
(31) Ritchie, D. W.; Kemp, G. J. L. Protein docking using spherical polar fourier correlations. *Proteins: Struct. Func. Genet.* **2000**, *39*, 178−194.
(32) Pérez-Nueno, V. I.; Ritchie, D. W.; Borrell, J. I.; Teixidó, J. Clustering and classifying diverse HIV entry inhibitors using a novel consensus shape based virtual screening approach: Further evidence for multiple binding sites within the CCR5 extracellular pocket. *J. Chem. Inf. Model.* **2008**, *48*, 2146−2165.
(33) International Union of Biochemistry and Molecular Biology, Nomenclature Committee & Webb, E.C. *Enzyme Nomenclature 1992: Recommendations of the Nomenclature Committee of the International Union Of Biochemistry and Molecular Biology on the Nomenclature and Classification of Enzymes*; Academic Press: San Diego, 1992.
(34) *LigPrep*, version 2.5, Schrödinger, LLC: New York, 2011.
(35) *Corina*, version 3.4, Corina Molecular Networks, GmbH Computerchemie Langemarckplatz 1: Erlangen, Germany, 2000.
(36) Sheridan, R. P.; Kearsley, S. K. Why do we need so many chemical similarity search methods? *Drug Discovery Today* **2002**, *7*, 903−911.
(37) Ben-Dor, A.; Shamir, R.; Yakhini, Z. Clustering gene expression patterns. *J. Comput. Biol.* **1999**, *6*, 281−297.
(38) Hodgkin, E. E.; Richards, W. G. Molecular similarity based on electrostatic potential and electric field. *Int. J. Quantum Chem. Quantum Biol. Symp.* **1987**, *14*, 105−110.
(39) Boys, S. F. Electronic wave functions. I. A general method of calculation for the stationary states of any molecular system. *Proc. Roy. Soc.* **1950**, *A200*, 542−555.
(40) *R: A Language and Environment for Statistical Computing*. R Development Core Team, R Foundation for Statistical Computing, Vienna, Austria, 2011. http://www.R-project.org (accessed February 5, 2012).
(41) Bratoeff, E.; Ramírez, E.; Murillo, E.; Flores, G.; Cabeza, M. Steroidal antiandrogens and 5alpha-reductase inhibitors. *Curr. Med. Chem.* **1999**, *6*, 1107−1123.
(42) Hasegawa, H.; Meeusen, R.; Sarre, S.; Diltoer, M.; Piacentini, M. F.; Michotte, Y. Acute dopamine/norepinephrine reuptake inhibition increases brain and core temperature in rats. *J. Appl. Physiol.* **2005**, *99*, 1397−1401.
(43) Bai, A.-P.; Ouyang, Q.; Zhang, W.; Wang, C. H.; Li, S.-F. Probiotics inhibit TNF-alpha-induced interleukin-8 secretion of HT29 cells. *World J. Gastroenterol.* **2004**, *10*, 455−457.
(44) Fiedler, M. A.; Wernke-Dollries, K.; Stark, J. M. Inhibition of TNF-alpha-induced NF-kappaB activation and IL-8 release in A549 cells with the proteasome inhibitor MG-132. *Am. J. Respir. Cell Mol. Biol.* **1998**, *19*, 259−268.
(45) Lee, E.; Robertson, T.; Smith, J.; Kilfeather, S. Leukotriene receptor antagonists and synthesis inhibitors reverse survival in eosinophils of asthmatic individuals. *Am. J. Respir. Crit. Care Med.* **2000**, *161*, 1881−18816.
(46) Robinson, A. J.; Kashanin, D.; O'Dowd, F.; Williams, V.; Walsh, G. M. Montelukast inhibition of resting and GM-CSF-stimulated eosinophil adhesion to VCAM-1 under flow conditions appears independent of cysLT$_1$R antagonism. *J. Leukocyte Biol.* **2008**, *83*, 1522−1529.
(47) Bernstein, J. A.; Greenberger, P. A.; Patterson, R.; Glass, M.; Krell, R.; Thyrum, P. T. The effect of the oral leukotriene antagonist, ICI 204,219, on leukotriene D4 and histamine-induced cutaneous vascular reactions in man. *J. Allergy Clin. Immunol.* **1991**, *87*, 93−98.
(48) Miyazaki, T.; Honda, K.; Ohata, H. Requirement of Ca_2^+ influx- and phosphatidylinositol 3-kinase-mediated m-calpain activity for shear stress-induced endothelial cell polarity. *Am. J. Physiol. Cell Physiol.* **2007**, *293*, C1216−C1225.
(49) Gomez-Cambronero, J.; Wang, E.; Johnson, G.; Huang, C.-H.; Sha'afiil, R. I. Platelet-activating factor induces tyrosine phosphorylation in human neutrophils. *J. Biol. Chem.* **1991**, *266*, 6240−6245.
(50) Shen, T. Y.; Goldstein, D.; Gingrich, D. M. Neolignan Derivatives as Platelet Activating Factor Receptor Antagonists and 5-Lipoxygenase Inhibitors. U.S. Patent 5639782, January 3, 1994.
(51) Lagente, V.; Moodley, I.; Perrin, S.; Mottin, G.; Junien, J.-L. Effects of isozyme-selective phosphodiesterase inhibitors on eosinophil infiltration in the guinea-pig lung. *Eur. J. Pharmacol.* **1994**, *255*, 253−256.
(52) Asako, H.; Wolf, R. E.; Granger, D. N. Leukocyte adherence in rat mesenteric venules: Effects of adenosine and methotrexate. *Gastroenterolog.* **1993**, *104*, 31−37.
(53) Mest, H.-J.; Hörhold, I.; Reina, T.; Riedela, A.; Broquet, C. Effect of BN 52256 and other mediator antagonists on ouabain-induced cardiac arrhythmia in a model of anaphylaxis in guinea-pigs. *Pharmacol. Res.* **1992**, *25*, 173−180.
(54) Pedersen, S. B.; Kristensen, K.; Richelsen, B. Anti-glucocorticoid effects of progesterone in vivo on rat adipose tissue metabolism. *Steroids* **2003**, *68*, 543−550.
(55) Kaiser, N.; Mayer, M.; Milholland, R. J.; Rosen, F. Studies on the antiglucocorticoid action of progesterone in rat thymocytes: Early in vitro effects. *J. Steroid Biochem.* **1979**, *10*, 379−386.
(56) Chen, T. C.; Kittaka, A. Novel vitamin D analogs for prostate cancer therapy. *ISRN Urol.* [Online] **2011**, Article ID 301490. http://www.ncbi.nlm.nih.gov/pubmed/22084796 (accessed June 11, **2012**).
(57) Llach, F.; Keshav, G.; Goldblat, M. V.; Lindberg, J. S.; Sadler, R.; Delmez, J.; Arruda, J.; Lau, A.; Slatopolsky, E. Suppression of parathyroid hormone secretion in hemodialysis patients by a novel vitamin D analogue: 19-Nor-1,25-dihydroxyvitamin D2. *Am. J. Kidney Dis.* **1998**, *32*, S48−S54.
(58) Hamilton-Miller, J. M. T. β-Lactams: Variations on a chemical theme, with some surprising biological results. *J. Antimicrob. Chemother.* **1999**, *44*, 729−734.
(59) Struss, D.; Storck, J.; Zimmermann, R. E. The inhibition of thrombin and chymotrypsin by heparin-cofactor II. *Thromb. Res.* **1992**, *68*, 45−56.
(60) Albano, S. M.; Lima, A. S.; Miguel, M. G.; Pedro, L. G.; Barroso, J. G.; Figueiredo, A. C. Antioxidant, anti-5-lipoxygenase and antiacetylcholinesterase activities of essential oils and decoction waters of some aromatic plants. *Rec. Nat. Prod.* **2012**, *6*, 35−48.
(61) Mizumoto, A.; Itoh, Z. Effects of 5-hydroxytryptamine 3 receptor antagonists on gastrointestinal motor activity in conscious dogs. *Nihon Heikatsukin Gakkai Zasshi.* **1989**, *25*, 155−165.
(62) Ramirez, M. J.; DelRio, J.; Cenarruzabeitia, E.; Lasheras, B. On the nature of the 5-HT receptor subtype inhibiting acetylcholine release in the guinea-pig ileum. *Br. J. Pharmacol.* **1994**, *113*, 77−80.
(63) Bengmark, S. Curcumin: An atoxic antioxidant and natural NF-κB, COX-2, LOX and iNOS inhibitor-a shield against acute and chronic disease. *J. Parenter. Enteral. Nutr.* **2006**, *30*, 45−51.
(64) Elliott, K.; Minami, N.; Kolesnikov, Y. A.; Pasternak, G. W.; Inturrisi, C. E. The NMDA receptor antagonists, LY274614 and MK-801, and the nitric oxide synthase inhibitor, NG-nitro-L-arginine, attenuate analgesic tolerance to the mu-opioid morphine but not to kappa opioids. *Pain* **1994**, *56*, 69−75.
(65) Endres, M.; Scott, G.; Namura, S.; Salzman, A. L.; Huang, P. L.; Moskowitz, M. A.; Szabó, C. ole of peroxynitrite and neuronal nitric oxide synthase in the activation of poly(ADP-ribose) synthetase in a murine model of cerebral ischemia-reperfusion. *Neurosci. Lett.* **1998**, *248*, 41−44.
(66) Ebert, D. H.; Deussing, J.; Peters, C.; Dermody, T. S. Cathepsin L and cathepsin B mediate reovirus disassembly in murine fibroblast cells. *J. Biol. Chem.* **2002**, *277*, 24609−24617.
(67) Carriere, J. L.; El-Fakahany, E. E. Choline is a full agonist in inducing activation of neuronal nitric oxide synthase via the muscarinic M_1 peceptor. *Pharmacology* **2000**, *60*, 82−89.
(68) Marino, M. J.; Rouse, S. T.; Levey, A. I.; Potter, L. T.; Conn, P. J. Activation of the genetically defined m1 muscarinic receptor potentiates N-methyl-D-aspartate (NMDA) receptor currents in

hippocampal pyramidal cells. *Proc. Natl. Acad. Sci. U.S.A.* **1998**, *95*, 11465−11470.
(69) Schwartz, J. C.; Arrang, J. M.; Garbarg, M. Histamine. In *Neuropsychopharmacology: The Fifth Generation of Progress*; Davis, K. L., Charney, D., Coyle, J. T., Nemeroff, C., Eds.; American College of Neuropsychopharmacology: Nashville, TN, 2002; Chapter 14.
(70) Starr, K. R.; Price, G. W.; Watson, J. M.; Atkinson, P. J.; Arban, R.; Melotto, S.; Dawson, L. A.; Hagan, J. J.; Upton, N.; Duxon, M. S. SB-649915-B, a novel 5-HT1A/B autoreceptor antagonist and serotonin reuptake inhibitor, is anxiolytic and displays fast onset activity in the rat high light social interaction test. *Neuropsychopharmacology* **2007**, *32*, 2163−2172.
(71) Schrattenholz, A. Muscarinic Antagonists with PARP and SIR Modulating Activity as Agents for Inflammatory Diseases. U.S. Patent 8039464, October 18, 2011.
(72) Scott, C.; Soffin, E. M.; Hill, M.; Atkinson, P. J.; Langmead, C. J.; Wren, P. B.; Faedo, S.; Gordon, L. J.; Price, G. W.; Bromidge, S.; Johnson, C. N.; Hagan, J. J.; Watson, J. SB-649915, a novel, potent 5-HT1A and 5-HT1B autoreceptor antagonist and 5-HT re-uptake inhibitor in native tissue. *Eur. J. Pharmacol.* **2006**, *536*, 54−61.
(73) Romero, L.; Artigas, F. Preferential potentiation of the effects of serotonin uptake inhibitors by 5-HT1A receptor antagonists in the dorsal raphe pathway: Role of somatodendritic autoreceptors. *J. Neurochem.* **1997**, *68*, 2593−2603.
(74) Sharp, T.; Umbers, V.; Gartside, S. E. Effect of a selective 5-HT reuptake inhibitor in combination with 5-HT1A and 5-HT1B receptor antagonists on extracellular 5-HT in rat frontal cortex in vivo. *Br. J. Pharmacol.* **1997**, *121*, 941−946.
(75) Cai, X.; Flores-Hernandez, J.; Feng, J.; Yan, Z. Activity-dependent bi-directional regulation of GABAA receptor channels by serotonin 5-HT4 receptors in pyramidal neurons of the prefrontal cortex. *J. Physiol. (London)* **2002**, *540*, 743−759.
(76) Bianchi, C.; Rodi, D.; Marino, S.; Beani, L.; Siniscalchi, A. Dual effects of 5-HT4 receptor activation on GABA release from guinea pig hippocampal slices. *Neuroreport* **2002**, *13*, 2177−2180.
(77) Li, C. Y.; Wang, H.; Xue, H.; Carlier, P. R.; Hui, K. M.; Pang, Y. P.; Li, Z. W.; Han, Y. F. Bis(7)-tacrine, a novel dimeric AChE inhibitor, is a potent GABA(A) receptor antagonist. *Neuroreport* **1999**, *10*, 795−800.
(78) Huidobro-Toro, J. P.; Valenzuela, C. F.; Harris, R. A. Modulation of GABAA receptor function by G protein-coupled 5-HT2C receptors. *Neuropharmacology* **1996**, *35*, 1355−1363.
(79) Fink, K. B.; Göthert, M. *Pharmacol. Rev.* **2007**, *59*, 360−417.
(80) Wood, M. D.; Heidbreder, C.; Reavill, C.; Ashby, C. R., Jr.; Middlemiss, D. N. Enhanced 5-HT2C receptor signaling is associated with haloperidol-induced "early onset" vacuous chewing in rats: Implications for antipsychotic drug therapy. *Drug Dev. Res.* **2001**, *54*, 88−94.
(81) Rudolph, U.; Knoflach, F. Beyond classical benzodiazepines: Novel therapeutic potential of GABAA receptor subtypes. *Nat. Rev. Drug. Discovery* **2011**, *10*, 685−697.
(82) Phebus, L. A.; Johnson, K. W.; Zgombick, J. M.; Gilbert, P. J.; Van Belle, K.; Mancuso, V.; Nelson, D. L.; Calligaro, D. O.; Kiefer, A. D., Jr.; Branchek, T. A.; Flaugh, M. E. Characterization of LY344864 as a pharmacological tool to study 5-HT1F receptors: Binding affinities, brain penetration and activity in the neurogenic dural inflammation model of migraine. *Life Sci.* **1997**, *61*, 2117−2126.
(83) Hopkins, A.; Mason, J. S.; Overington, J. P. How many drug targets are there? *Curr. Opin. Struct. Biol.* **2006**, *16*, 127−136.
(84) Castel, H.; Louiset, E.; Anouar, Y.; Le Foll, F.; Cazin, L.; Vaudry, H. Regulation of GABAA receptor by protein tyrosine kinases in frog pituitary melanotrophs. *J. Neuroendocrinol.* **2000**, *12*, 41−52.
(85) Tabrizchi, R. Dual ACE and neutral endopeptidase inhibitors: Novel therapy for patients with cardiovascular disorders. *Drugs* **2003**, *63*, 2185−2204.
(86) Rolin, S.; Petein, M.; Tchana-Sato, V.; Dogne, J. M.; Benoit, P.; Lambermont, B.; Ghuysen, A.; Kolh, P.; Masereel, B. BM-573, a dual thromboxane synthase inhibitor and thromboxane receptor antagonist, prevents pig myocardial infarction induced by coronary thrombosis. *J. Pharmacol. Exp. Ther.* **2003**, *306*, 59−65.
(87) Brownlie, R. P.; Brownrigg, N. J.; Butcher, H. M.; Garcia, R.; Jessup, R.; Lee, V. J.; Tunstall, S.; Wayne, M. G. ZD1542, a potent thromboxane A2 synthase inhibitor and receptor antagonist in vitro. *Br. J. Pharmacol.* **1993**, *110*, 1600−1606.
(88) Kontogiorgis, C.; Hadjipavlou-Litina, D. Thromboxane synthase inhibitors and thromboxane A2 receptor antagonists: A quantitative structure activity relationships (QSARs) analysis. *Curr. Med. Chem.* **2010**, *17*, 3162−3214.
(89) Stahl, S. M.; Pradko, J. F.; Haight, B. R.; Modell, J. G.; Rockett, C. B.; Learned-Coughlin, S. A review of the neuropharmacology of bupropion, a dual norepinephrine and dopamine reuptake inhibitor. *J. Clin. Psychiatry* **2004**, *6*, 159−166.
(90) Farber, N. B.; Hanslick, J.; Kirby, C.; McWilliams, L.; Olney, J. W. Serotonergic agents that activate 5HT2A receptors prevent NMDA antagonist neurotoxicity. *Neuropsychopharmacology* **1998**, *18*, 57−62.